THE EFFECT OF RAINFALL SEQUENCING ON EROSION DYNAMICS: A LARGE SCALE RAINFALL SIMULATION EXPERIMENT

Jantiene Baartman (1), Niels Lake (1), Bart Verschaeren (1), Hannah Williams (2), Stuart McLelland (2), Dan Parsons (3) & Martine van der Ploeg (1)

(1) Soil Physics and Land Management Group, Wageningen University, the Netherlands, E-mail: jantiene.baartman@wur.nl
(2) Department of Geography, Geology and Environment, University of Hull, UK Hull University
(3) Energy and Environment Institute, University of Hull, UK Hull University

Climate change is expected to result in more extreme rainfall events, which may impact soil erosion rates and patterns. Adaptation is difficult if the effects are unknown, especially as the magnitude-frequency relationship is highly non-linear and may also depend on connected pathways within a landscape. Both were investigated in the Total Environment Simulator at Hull University in a large-scale rainfall simulation experiment. Erosion effects on plots with two grain sizes, and five different rainfall events in varying order were combined for a total of 10 sequences. The results show highly variable responses. Further work will focus on quantifying DEMs of difference to determine the connectivity of the two plots in relation to the different sequences of rainfall events.

1. INTRODUCTION

Although research and interventions have aimed at soil and water conservation (Panagos et al. 2015), erosion by water is still a large threat to soils globally (EU 2006, Pimentel 2006). The effects of soil and water conservation efforts are difficult to estimate, because of the non-linearity in the relationship between rainfall, runoff and erosion (Boardman et al. 1999, Philips 2003, Cerdà et al. 2013) and differences across scales (Cammeraat 2004, Cantón et al. 2011 Vanmaerke et al. 2011). This non-linearity is known from field and model studies of catchments; precipitation events with higher amounts of rainfall do not necessarily produce greater amounts of eroded material, similarly lower amounts of rainfall do not necessarily produce less eroded material (Gonzalez-Hidalgo 2007, Hungr et al. 2008, Van de Wiel et al., Baartman et al. 2013a). Even if low amounts of rainfall produce less erosion, these low amounts of rainfall may occur more frequently compared to extreme events, potentially leading to a higher net amount of soil loss (Marques et al. 2007). This so-called magnitude-frequency relation is not yet established, since data and information on this relation is limited.

One of the reasons the magnitude-frequency relationship is not clear, is the lack of repeatability in real landscapes. Once a rainfall event has occurred, the landscape has changed, and therefore no consistent testing of the magnitude-frequency relationship is possible.

Hence, the most pressing issue currently is the lack of data on both rainfall event information and the response of a landscape in terms of soil loss to sequences of rainfall events (González-Hidalgo et al. 2009). Nonetheless, in numerical modelling studies it is possible to recreate the exact same landscape. A modeling study by Baartman et al. (2013a) showed no particular trends for 50 varying rainfall events. Possibly, the lack of particular trends is caused by another factor, namely the change in connectivity in a landscape (Appels et al. 2011, Baartman et al. 2013b, Bracken et al. 2013). If pathways in a landscape suddenly connect during a particular rainfall event, sediment may leave a catchment as a sudden pulse (Schoorl et al. 2014).

As a result of climate change, it can be expected that the frequency-magnitude of rainfall events will change, most likely extreme rainfall events will become more intense and frequent in many regions (IPCC, 2014), leading to accelerated erosion and flooding. However, adaptation to such changes is not possible, if their effects are unknown. Therefore, analysis of the possible effects of rainfall event sequence with different magnitude-frequency occurrence on landscape dynamics, including erosion and sediment dynamics is an urgent research task (Boardman, 2006). This research aimed to improve our understanding of the effects of different sequences of rainfall events on erosion and sediment dynamics. The Total Environment Simulator at the University of Hull was ideally suited for this research, offering a large experimental area in which a small 'landscape' could be imitated and recreated to test the effects of varying rainfall event sequences.

2. MATERIALS AND METHODS

The 'Total Environment Simulator' (TES, at Hull University, UK, was used for the rainfall simulation experiments. The TES consists of a surface area of ~40 m^2 and is equipped with a rainfall simulation system containing 40 rainfall nozzles arranged in a regular grid above the experimental area (Fig. 1).

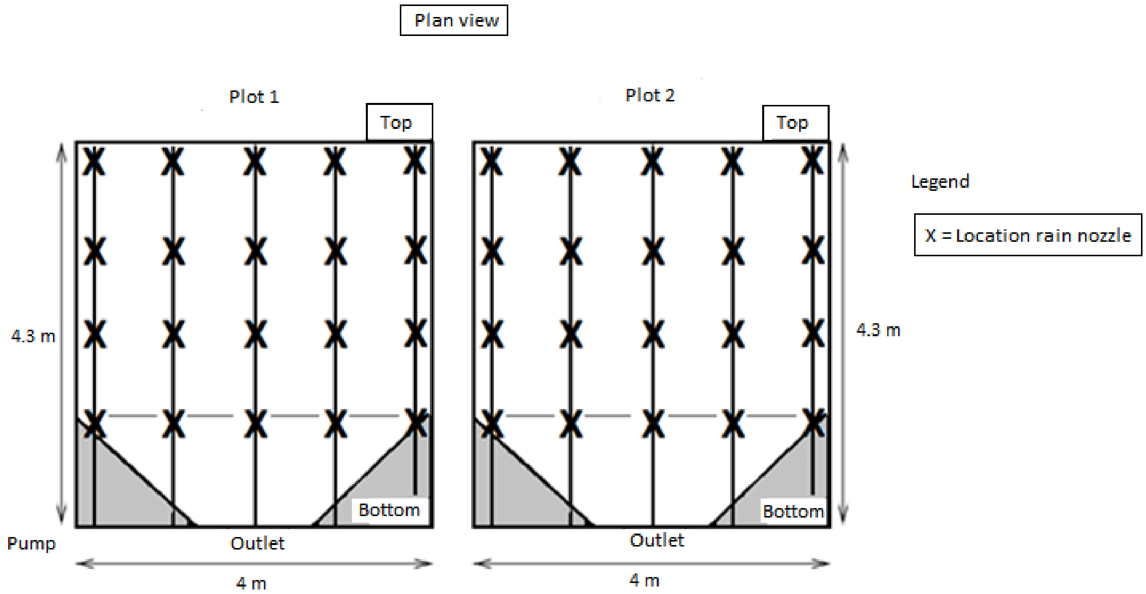

Figure 1: Schematic overview of the rainfall nozzle system over the experimental plots in the TES.

The experimental design consisted of two plots (plot 1, left hand and plot two, right hand in Fig. 1) of 4 by 4.3 m. Each plot was filled with different size sand: plot 1 contained fine sand (D50 = 215 µm) and plot 2 contained medium coarse sand (D50 = 458 µm). Grainsize distribution within the plots was uniform. The base of each plot was sealed with an impermeable plastic layer to avoid leakage of infiltrating water. The plots had the same morphology with a V-shape in the upper part, resulting in an inward flow direction towards the middle of the plot and an almost straight (very slightly V-shaped) slope downwards towards the outlet in the lower part of the plot. Dimensions and slopes are given in Fig. 2a and b for plot 1 and 2 respectively.

a.

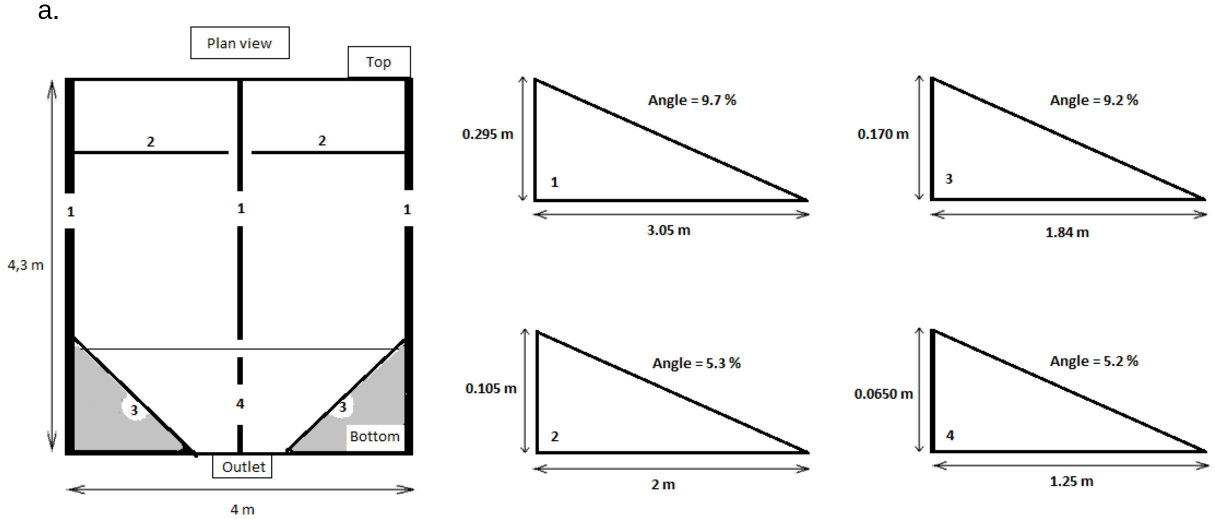

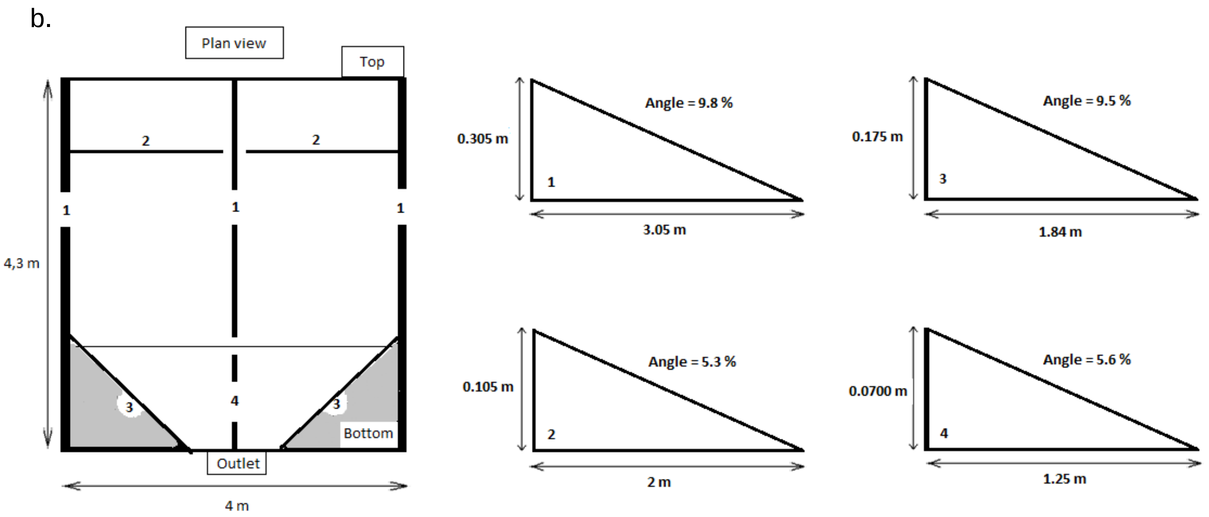

Figure 2: Design of plots 1 (a) and plot 2 (b) including dimensions and slopes.

Before the rainfall sequences could be designed, the rainfall simulation system was tested and calibrated. To calibrate the rainfall intensities and to investigate the spatial variation of the rainfall within each plot, 22 rain gauges and 27 boxes were installed on each plot (Fig. 3a). As shown in Fig. 3b, the rainfall was not spatially uniformly distributed.

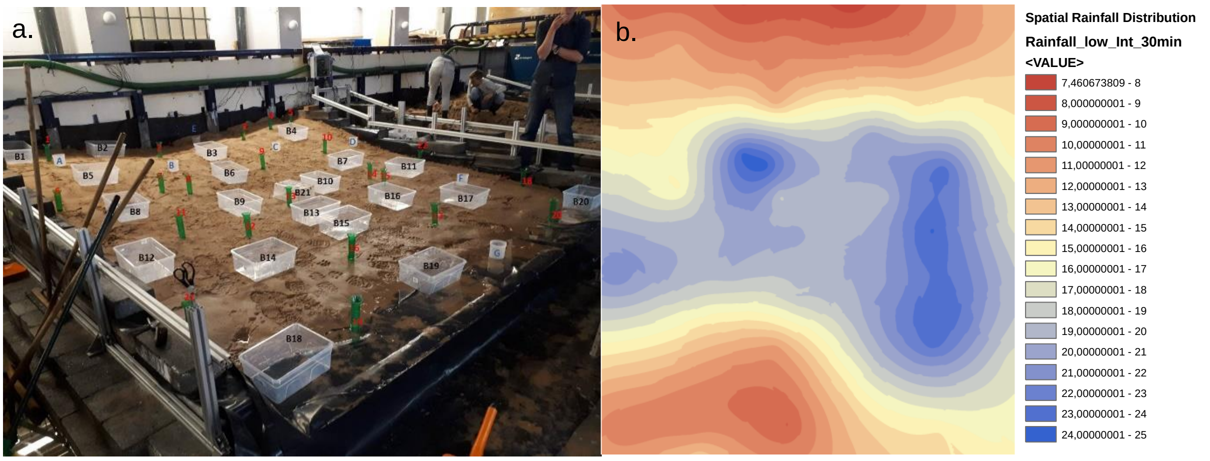

Figure 3: a) Calibration set-up to calibrate the rainfall distribution over the experimental plot, b) interpolated spatial distribution of rainfall of the low intensity rainfall event (Photo: Niels Lake / Bart Verschaeren).

From several tests, eventually it was decided to use three rainfall intensities (Table 1) of significant difference: Low (35 and 33 mm/h), Medium (92 and 78 mm/h) and High (126 and 117 mm/h for plot 1 and plot 2 respectively). Higher intensities were not possible due to the pumping capacity of the system, while lower intensities led to dripping of the system, with unwanted large drops being produced by the nozzles. The spatially averaged rainfall intensities are consistently lower for plot 2 as compared to plot 1, due to a slightly decreasing water pressure with increasing distance from the water pump, which was located closer to plot 1.

Table 1 Calibrated average rainfall intensities for plot 1 and plot 2

Rainfall Intensity	Low (mm/h)	Medium (mm/h)	High (mm/h)
Plot 1	35.1	92.1	126
Plot 2	33.0	79.4	117

A total of 10 sequences of rainfall events were applied to both plots. Rainfall sequences consisted of the same 5 individual rainfall events (Table 2), but applied in different order (Table 3). One of the sequences was the so-called ‘base sequence’ which consisted of 5 events of the same intensity and duration. To ensure an equal total amount of rainfall being applied as in the other sequences, the duration of each event was 19 minutes.

Table 2: Rainfall events: intensity and duration.

Rainfall event code	Intensity			Duration (min)
		Plot 1 (mm/h)	Plot 2 (mm/h)	
1 - L30	Low	35	33	30
2 - L60	Low	35	33	60
3 - M15	Medium	92	78	15
4 - M30	Medium	92	78	30
5 - H15	High	126	117	15

Table 3: Sequences of rainfall events applied to the plots, codes as in Table 2.

Sequence	**1**	**2**	**3**	**4**	**5**	**6**	**7**	**8**	**9**	**10**
event.ID	**Increasing**	**Decreasing**	**Hill**	**Valley**	**Stabilizing**	**Destabilizing**	**Base run**	**Random1**	**Random2**	**Random3**
A	**L30**	**H15**	**L30**	**M30**	**H15**	**L30**	**M19**	**L30**	**M15**	**L60**
B	**L60**	**M30**	**M30**	**L60**	**L30**	**L60**	**M19**	**M30**	**L30**	**L30**
C	**M15**	**M15**	**H15**	**L30**	**M30**	**M30**	**M19**	**M15**	**L60**	**H15**
D	**M30**	**L60**	**M15**	**M15**	**L60**	**L30**	**M19**	**H15**	**H15**	**M15**
E	**H15**	**L30**	**L60**	**H15**	**L30**	**H15**	**M19**	**L30**	**M30**	**M30**

To be able to compare the effects of the different rainfall sequences, the starting landscape needed to be the same. Therefore, the plots were (re)built each time to the same morphology as much as possible. The topsoil was loosened with a rake to remove channels and patterns formed by a previous sequence. The soil was then compacted, while care was taken to do this as homogeneously as possible over the plot surface. Finally, a scraping board specifically made for this experiment was used to recreate the same slope and landscape form. To minimize differences in the effects of the rainfall events due to differences evolving from the tramping and scraping phase, a spin-up rainfall event was applied before each rainfall sequence. The spin-up event was a low intensity, one-hour rainfall event. Figure 4 and 5 show the difference in the plot surface before and after applying the spin-up event.

Figure 4. Smooth landscape after scraping phase (plot 1).

Figure 5. Starting landscape after spin-up rainfall event (plot 1).

At the outlet of each plot, a large box was placed to collect the runoff water and sediment during each rainfall event. The runoff water was automatically measured by directing it into large containers placed on scales. The sediment was manually collected from the boxes after each rainfall event and weighted. A conversion factor from wet to dry sediment was calibrated and applied to convert the weighed wet sediment to dry sediment weight. From three starting landscapes, bulk density samples were taken at top, middle and low positions in the plot using 100

cm^3 sample rings. These were used to check if rebuilding of the plots leads to differences in bulk density. Soil moistures sensors (EC5) were installed in the plots to check the spatial distribution and temporal evolution of soil moisture during the experiment. Finally, after each rainfall event, the surface was scanned using a FARO X330 high-resolution laser scanner.

3. RESULTS & DISCUSSION

During the experiment surface runoff caused by field saturation was observed for both grain sizes. Spatial differences in erosion patterns between both plots were clearly visible (Fig. 6).

Figure 6. Typical erosion pattern for plot 1 with fine sand (left) and plot 2 with medium sand (right).

Figure 7 and 8 show the erosion amounts for the two plots generated by each rainfall event within each sequence executed in the experiment. Sequences are indicated by the different colors. Rainfall event size (Table 2), is indicated from small to large with increasing circle size. The order of occurrence of events 1-5 in a sequence is indicated as A to E on the x-axis. As can be seen, the results for this experiment were very heterogeneous.

From the overview of plot 1 (Fig. 7), clear differences can be distinguished in the amount of erosion between the lower three rainfall event numbers (events 1, 2 and 3) and the two higher rainfall event numbers (events 4 and 5). The highest erosion value of these first three event numbers is 8.19 kg, while the lowest erosion value of event 4 and 5 is 11.57 kg. Furthermore, when event 1 or event 5 is the first event in a sequence, the subsequent amount of erosion generated by this event is the lowest for this specific rain event. When events 1 and 5 are run later in the sequence, e.g. on timestep B, C, D or E, the amount of erosion is always higher. Also, event 1 generates the lowest amount of erosion in all sequences; erosion generated by the other events is always higher.

Plot 2 shows (Fig. 8) that event 1 and event 5 generate, similar to plot 1, the lowest erosion amounts when located as the first event in a sequence. There is one exception for event 5 in sequence 5, which has a higher erosion output compared to some other rainfall events of event 5. Also, event 1 is for all sequences generating the lowest amount of erosion. Other deviations can be seen from event 5 of sequence 2, which has less erosion compared to event 2 (sequence 10) or event 3 (sequence 9). For all other sequences, event 4 and 5 have the highest erosion amounts. Also, ranges in erosion are increasing from event C onwards, where maximum erosion reaches to around 15 kg compared to maximums of 9.35 kg for event A and 11.19 kg for event B.

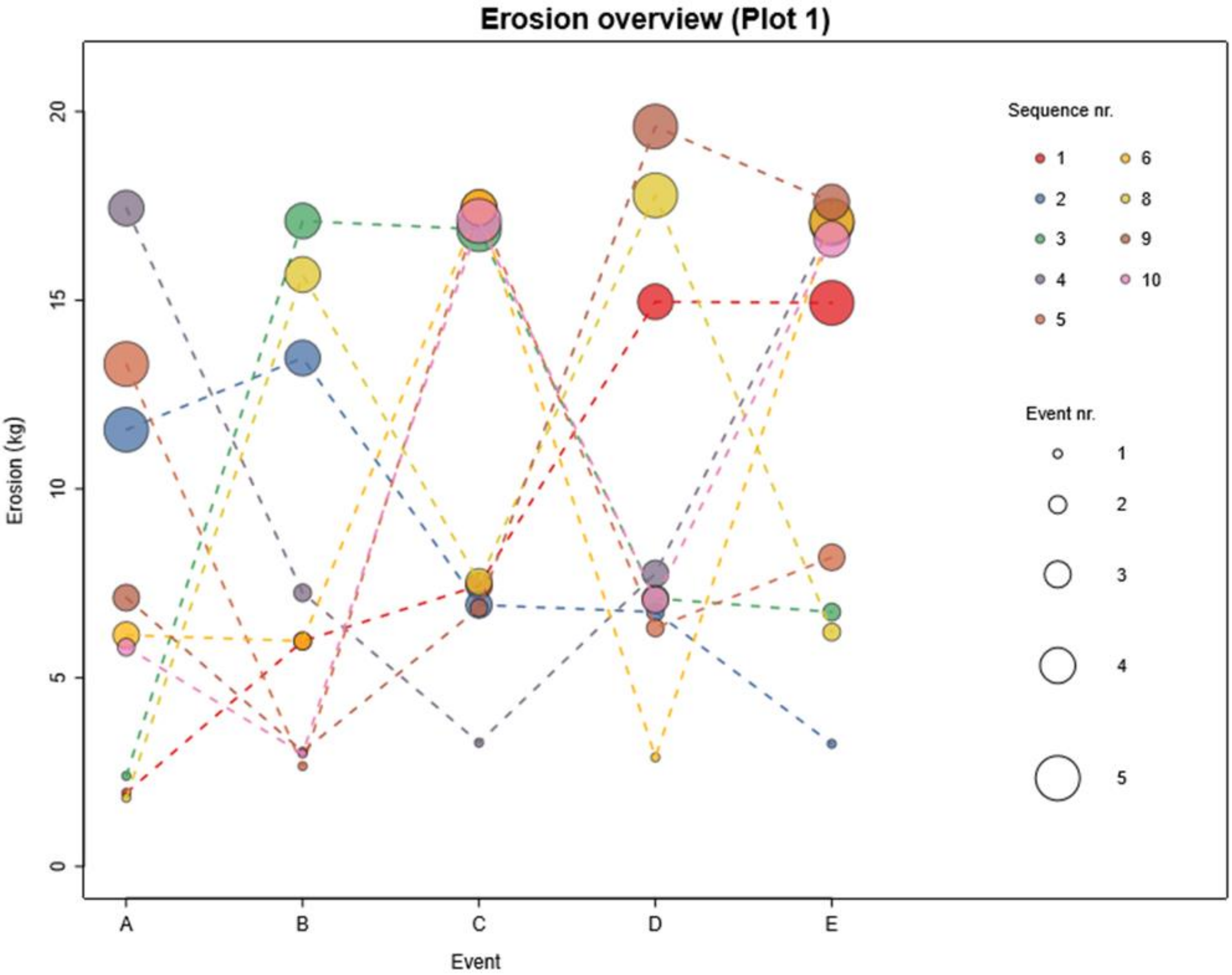

Figure 7. Erosion overview plot 1. Each color indicates one of the 10 sequences. Each circle size indicates one of the five rainfall events, where rainfall event 1 has the smallest circle and event 5 is indicated by the largest circle size.

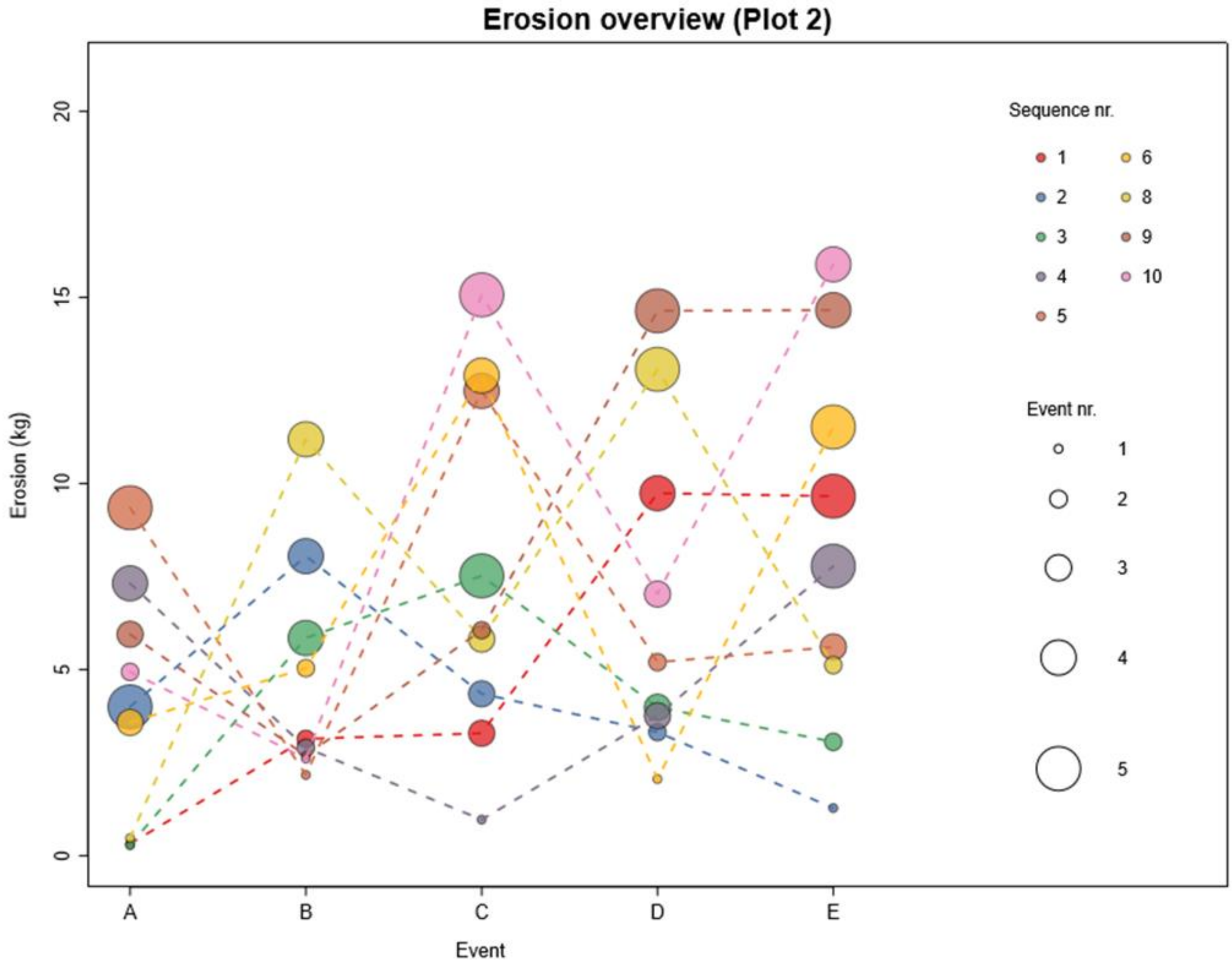

Figure 8. Erosion overview plot 2. Each color indicates one of the 10 sequences. Each circle size indicates one of the five rainfall events, where rainfall event 1 has the smallest circle and event 5 is indicated by the largest circle size.

Figures 9 and 10 show some first results of the analysis of the laser scan data for plot 1 and plot 2 respectively. The left-hand column of the figures (Fig. 9abc and 10abc) show results from after the spin-up event, so before application of a particular rainfall sequence, the right hand column (Fig. 9def and 10def) show results after the last event of a sequence of rainfall events. The figures show results of sequence 10. As can be seen from the pictures, and also from the slope patterns and flow accumulation patterns, a drainage pattern clearly developed due to the rainfall events. The slope maps show that rills developed in the upper part of the plot and the flow accumulation maps show that the drainage pattern development was mainly in the lower part of the plot. Comparing Figures 9 and 10, the flow pattern development in plot 2 (medium coarse sand) was somewhat wider as compared to the flow pattern development in plot 1 (fine sand), which is a bit more confined, especially in the middle of the plot. These differences in pattern development need to be analyzed in further detail.

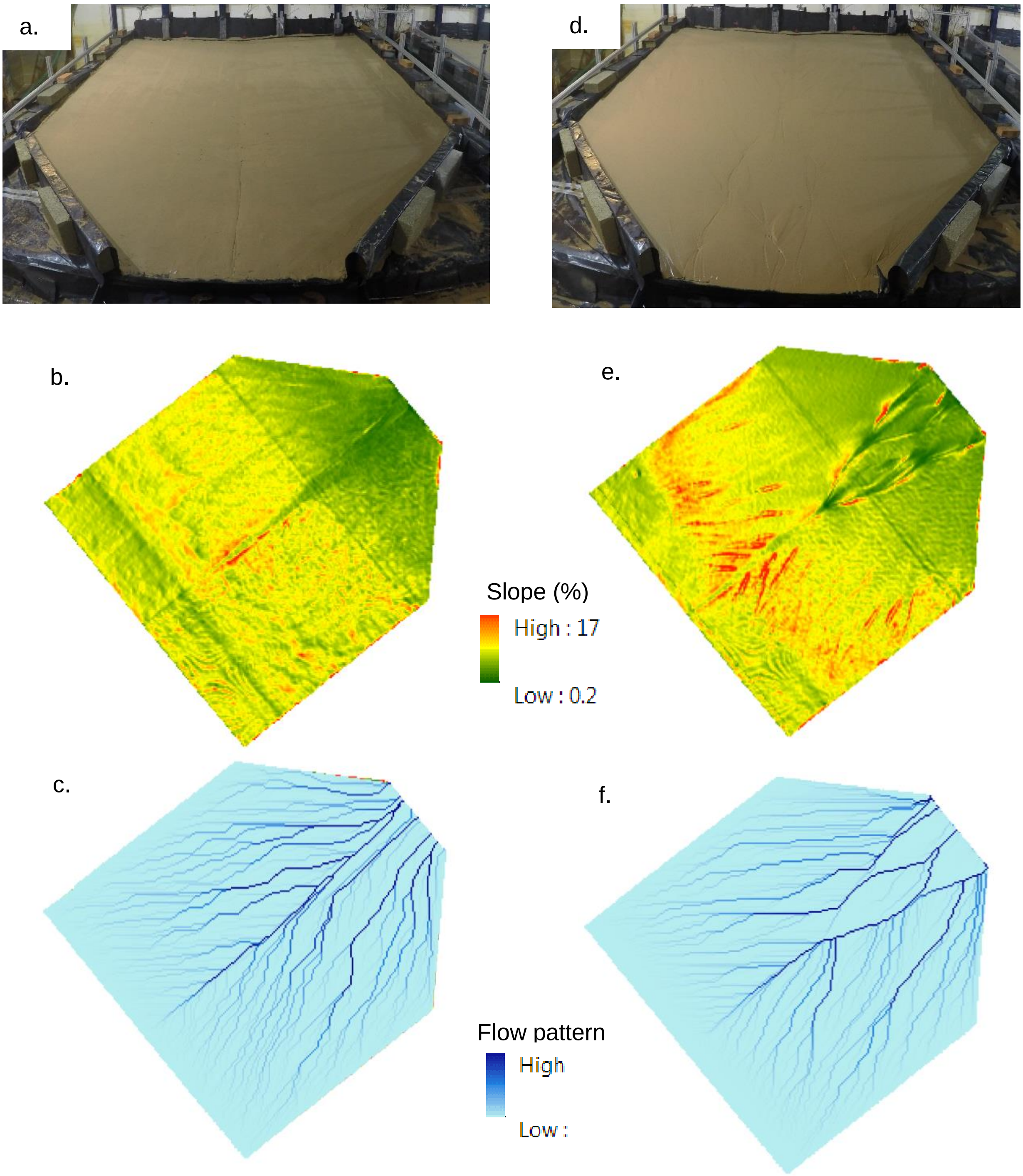

Figure 9. Pictures, slope maps and flow accumulation maps showing slope and flow pattern development between the beginning of sequence 10 (i.e. after spin-up; a,b,c) and at the end of sequence 10 (d,e,f) for plot 1.

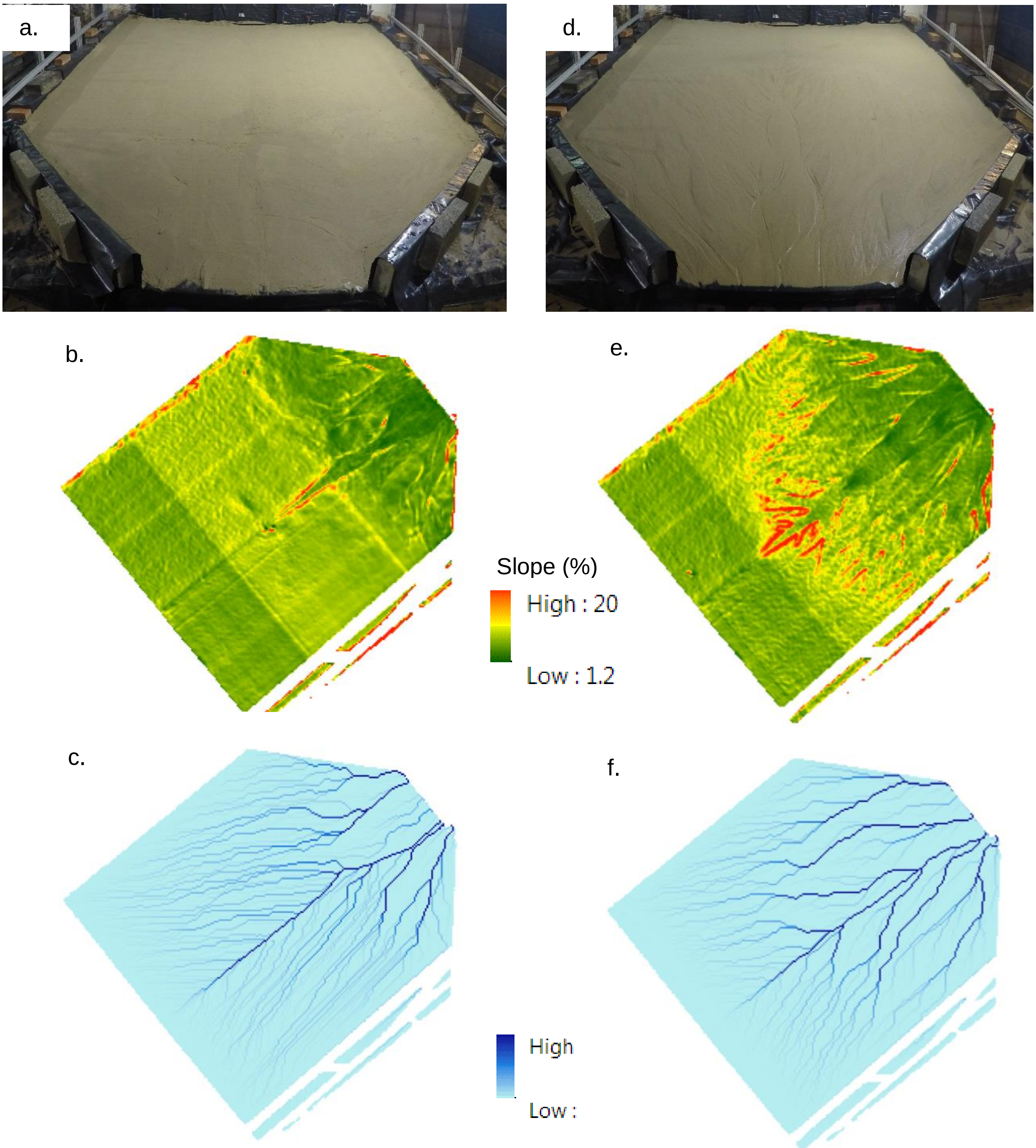

Figure 10. Pictures, slope maps and flow accumulation maps showing slope and flow pattern development between the beginning of sequence 10 (i.e. after spin-up; a,b,c) and at the end of sequence 10 (d,e,f) for plot 2.

4. OUTLOOK

In section 3, the current results of the project are presented. Further data processing and analysis is ongoing Some challenges have been encountered with post-processing of the laser scan data into reliable DEMs and DEMs of Difference (DoDs). When these challenges are solved, this data will be used to quantify connectivity development in the catchments. Subsequently, differences in connectivity development and patterns will be related to differences in erosion and sediment yield as measured from the different rainfall sequences. Furthermore, the data can be used to parameterize, calibrate and validate erosion and/or landscape evolution models (e.g. LAPSUS or CEASAR). These can then be used to evaluate erosion dynamics for different landscapes and (climate) scenarios.

ACKNOWLEDGEMENT

This project has received funding from the European Union's Horizon 2020 research and innovation programme under grant agreement No 654110, HYDRALAB+.

REFERENCES

Appels WM, Bogaart PW, van der Zee SEATM. 2011. Influence of spatial variations of microtopography and infiltration on surface runoff and field scale hydrological connectivity. *Advances in Water Resources* 34: 303-313. http://dx.doi.org/10.1016/j.advwatres.2010.12.003.

Baartman JEM, Temme AJAM, Veldkamp T, Jetten VG, Schoorl JM. 2013a. Exploring the role of rainfall variability and extreme events in long-term landscape development. *CATENA* 109: 25-38. http://dx.doi.org/10.1016/j.catena.2013.05.003.

Baartman JEM, Masselink R, Keesstra SD, Temme AJAM. 2013b. Linking landscape morphological complexity and sediment connectivity. *Earth Surface Processes and Landforms* 38: 1457-1471. 10.1002/esp.3434.

Boardman J. 2006. Soil erosion science: Reflections on the limitations of current approaches. *Catena* 68: 73-86.

Boardman J, Favis-Mortlock D. 1999. Frequency-magnitude distributions for soil erosion, runoff and rainfall – a comparative analysis. *Zeitschrift für Geomorphologie, Supplement band* 115: 51-70.

Bracken LJ, Wainwright J, Ali GA, Tetzlaff D, Smith MW, Reaney SM, Roy AG. 2013. Concepts of hydrological connectivity: Research approaches, pathways and future agendas. *Earth-Science Reviews* 119: 17-34. http://dx.doi.org/10.1016/j.earscirev.2013.02.001.

Cammeraat ELH. 2004. Scale dependent thresholds in hydrological and erosion response of a semi-arid catchment in southeast Spain. *Agriculture, Ecosystems & Environment* 104: 317-332.

Cantón Y, Solé-Benet A, de Vente J, Boix-Fayos C, Calvo-Cases A, Asensio C, Puigdefábregas J. 2011. A review of runoff generation and soil erosion across scales in semiarid south-eastern Spain. *Journal of Arid Environments* 75: 1254-1261.

Cerdà A, Brazier R, Nearing M, de Vente J. 2013. Scales and erosion. *CATENA* 102: 1-2. http://dx.doi.org/10.1016/j.catena.2011.09.006.

European Commission. 2006. Soil protection - the long story behind the strategy. Technical report. Office for Official Publications of the European Communities, Luxembourg.

Fryirs K. 2013. (Dis)Connectivity in catchment sediment cascades: a fresh look at the sediment delivery problem. *Earth Surface Processes and Landforms* 38: 30-46. 10.1002/esp.3242.

Gonzalez-Hidalgo JC, Pena-Monne JL, de Luis M. 2007. A review of daily soil erosion in Western Mediterranean areas. *Catena* 71: 193-199.

González-Hidalgo JC, de Luis M, Batalla RJ. 2009. Effects of the largest daily events on total soil erosion by rainwater. An analysis of the USLE database. *Earth Surface Processes and Landforms* 34: 2070-2077. 10.1002/esp.1892.

Hungr O, McDougall S, Wise M, Cullen M. 2008. Magnitude–frequency relationships of debris flows and debris avalanches in relation to slope relief. *Geomorphology* 96: 355-365. http://dx.doi.org/10.1016/j.geomorph.2007.03.020.

IPCC. 2014. *Climate Change 2014: Synthesis Report. Contribution of Working Groups I, II and III to the Fifth Assessment Report of the Intergovernmental Panel on Climate Change*. IPCC, Geneva, Switzerland:

Marques MJ, Bienes R, Jiménez L, Pérez-Rodríguez R. 2007. Effect of vegetal cover on runoff and soil erosion under light intensity events. Rainfall simulation over USLE plots. *Science of The Total Environment* 378: 161-165. http://dx.doi.org/10.1016/j.scitotenv.2007.01.043.

Panagos P, Borrelli P, Robinson DA. 2015. Common Agricultural Policy: Tackling soil loss across Europe. *Nature* 526: 195-195.

Phillips JD. 2003. Sources of nonlinearity and complexity in geomorphic systems. *Progress in Physical Geography* 27: 1-23. 10.1191/0309133303pp340ra.

Pimentel D. 2006. Soil erosion: A food and environmental threat. *Environment, Development and Sustainability* 8: 119-137. 10.1007/s10668-005-1262-8.

Schoorl JM, Temme AJAM, Veldkamp T. 2014. Modelling centennial sediment waves in an eroding landscape – catchment complexity. *Earth Surface Processes and Landforms* 39: 1526-1537. 10.1002/esp.3605.

Van De Wiel MJ, Coulthard TJ. 2010. Self-organized criticality in river basins: Challenging sedimentary records of environmental change. *Geology* 38: 87-90. 10.1130/G30490.1.

Vanmaercke M, Poesen J, Verstraeten G, de Vente J, Ocakoglu F. 2011. Sediment yield in Europe: Spatial patterns and scale dependency. *Geomorphology* 130: 142-161.